CFD-BASED SIMULATION AND MODEL VERIFICATION OF PEACHES FORCED AIR COOLING ON DIFFERENT AIR SUPPLY TEMPERATURES
/
基于CFD 的不同送风温度对蜜桃强制风冷的仿真与模型验证

Yingmin Chen, Haiyan Song*), Rui Zhao, Qin Su [1]
College of Agricultural Engineering, Shanxi Agricultural University, Taigu / China
Tel: +86-0354-6288316; E-mail: haiyansong2003@163.com, chenyingmin137@126.com
DOI: https://doi.org/10.35633/inmateh-63-06

***Keywords*:** *postharvest peach, computational fluid dynamics (CFD), forced air cooling (FAC), precooling, simulation, model verification*

ABSTRACT

To ensure optimum peach quality during precooling, air supply temperature within the precooled facility should be precisely controlled. Three-dimensional unsteady computational fluid dynamics (CFD) model was established in this research, taking air supply temperature as an influencing factor, a dynamic simulation of this model was performed based on Fluent, and its reliability was verified through experiments. Simulation results showed that the decrease of air supply temperature did not affect the 7/8ths cooling time (SECT) significantly, but shortened the cooling time of the fruit which was cooled from the initial temperature to a fixed temperature, especially when air supply temperature dropped below 4°C, its corresponding cooling time showed a trend of steady variation. Meanwhile, respiration rate of 6-8 °C was about twice as high as that of 2-4 °C, its corresponding moisture loss was also increased by 34.71-39.74%. Thus, the range of 2-4 °C was more suitable for quick precooling peaches after harvest. Experiments showed that the root mean square error (RMSE) of 0.7 and 2.7 m·s^{-1} were 0.747 and 0.836 °C, respectively. It could be seen that simulation results were in good agreement with experimental results, which fully verified the feasibility and high accuracy of this new modeling method. Finally, this study can provide a reliable reference for establishing an accurate precooling numerical model, and rationally optimizing air supply temperature range of fruits precooling experiment to maintain its high quality.

摘要

为保证蜜桃在预冷过程中的最佳品质，预冷设备内的送风温度须精确控制。本研究建立了三维果品非稳态的 CFD 数学仿真模型，以送风温度为影响因素，基于 Fluent 对该模型进行了动力学仿真，并通过实验进一步验证了该模型的可靠性。仿真结果表明：风温的减小并不会显著影响果品的 7/8 预冷时间，反而会缩短果品从初始温度降温至某一固定温度的冷却时间。当风温减小到低于 4℃时，其对应的冷却时间将呈现平稳变化的趋势，而且风温为 6-8 ℃时果品的呼吸速率约为 2-4 ℃的两倍，其水分损失量也增大了 34.71-39.74 %。由此可知，2-4 ℃的风温范围更适合蜜桃采后预冷。此外，模型验证实验表明：该模型在风温为 2 ℃时，0.7 和 2.7 m·s^{-1} 的仿真和实验的均方根误差分别为 0.747 和 0.836 ℃，模拟与实验结果的高度吻合充分证明了该新型建模方法的可行性和高准确性。该研究为建立高精准度预冷数值模型，合理优化果品预冷实验送风温度范围，保持其高品质提供了可靠的参考依据。

INTRODUCTION

Postharvest peach carries an amount of field heat, which makes the fruit breathe vigorously. According to the relevant statistics, the rate of quality loss is as high as 13 to 38% when the fruit reaches the consumers through the supply chain after harvest (*Kummu et al., 2012)*. Therefore, the most crucial step for freshly harvested fruits is to remove field heat via prompt precooling, which retards after-ripening and minimizes mass loss, prior to the refrigerated storage or transportation (*Becker et al., 2011; Wang et al., 2019)*. Moreover, forced-air cooling (FAC) is a typical and effective industrial postharvest handling technique.

During the forced-air cooling (FAC), the complexity of the air movement inside a single fruit-packing crate makes it difficult to measure temperature variations solely via field tests. More importantly, extending the test cycle requires significant human and material resources.

[1] *Yingmin Chen, As. Ph.D. Stud. Eng.; Haiyan Song*, Prof. Ph.D. Eng.; Rui Zhao, As. Ph.D. Stud. Eng.; Qin Su, As. M.E. Stud. Eng.*

However, these difficulties can be avoided by using computational fluid dynamics (CFD) to create a three- dimensional numerical model. This is because the transient coupling effect of fluid-solid can be simulated by CFD, and it can also obtain the distribution of airflow and temperature at a high spatiotemporal resolution (*Norton et al., 2007*). Therefore, actual measurements in experiments are required only at specific locations to verify the accuracy of the simulation. However, some of these models do not take into account the effect of these heat sources on heat flow inside the fruit zone *(Ferrua et al., 2008a and 2008b; Berry et al., 2016; Han et al., 2017)*, which leads to the reduced reliability of the simulation results from such studies. From this, a new modelling method is proposed to improve the accuracy of simulation results in peaches cooling, and these heat sources are coded as detailed procedures by a user-defined function (UDF) written in C programming language.

In addition, CFD has been widely applied to research the cooling phenomena of various horticultural food products for optimizing the design of precooling packing crates or finding the optimal air-inflow velocity (*Delele et al., 2013a and 2013b; Han et al., 2017).* Unfortunately, few studies have analysed the comprehensive effects of different air supply temperatures on postharvest peaches during precooling.

Therefore, the objective of this study is to determine the optimal range of air supply temperature and to verify the feasibility of this new modeling method. This modelling method can accurately predict the temporal and spatial temperature distribution in the fruit cooling process, and can also save an amount of manpower and material resources consumed in the precooling experiments, so that this method can be widely applied in precooling research. Moreover, this study does not only provide a new modelling method to simulate airflow and heat transfer for different precooling strategies during fruits cooling, but offers a reference for optimizing the air supply temperature range for improving the peaches precooling performances.

MATERIALS AND METHODS

Geometry and meshing

We used Design Modeler of ANSYS19.2 to create a packaging corrugated carton packed with three layers of peaches. The thickness of this container and trays were 7 and 4 mm, and the structure design was shown in Fig.1, among them, the tray was a single corrugated cardboard of 368×256 mm^2.

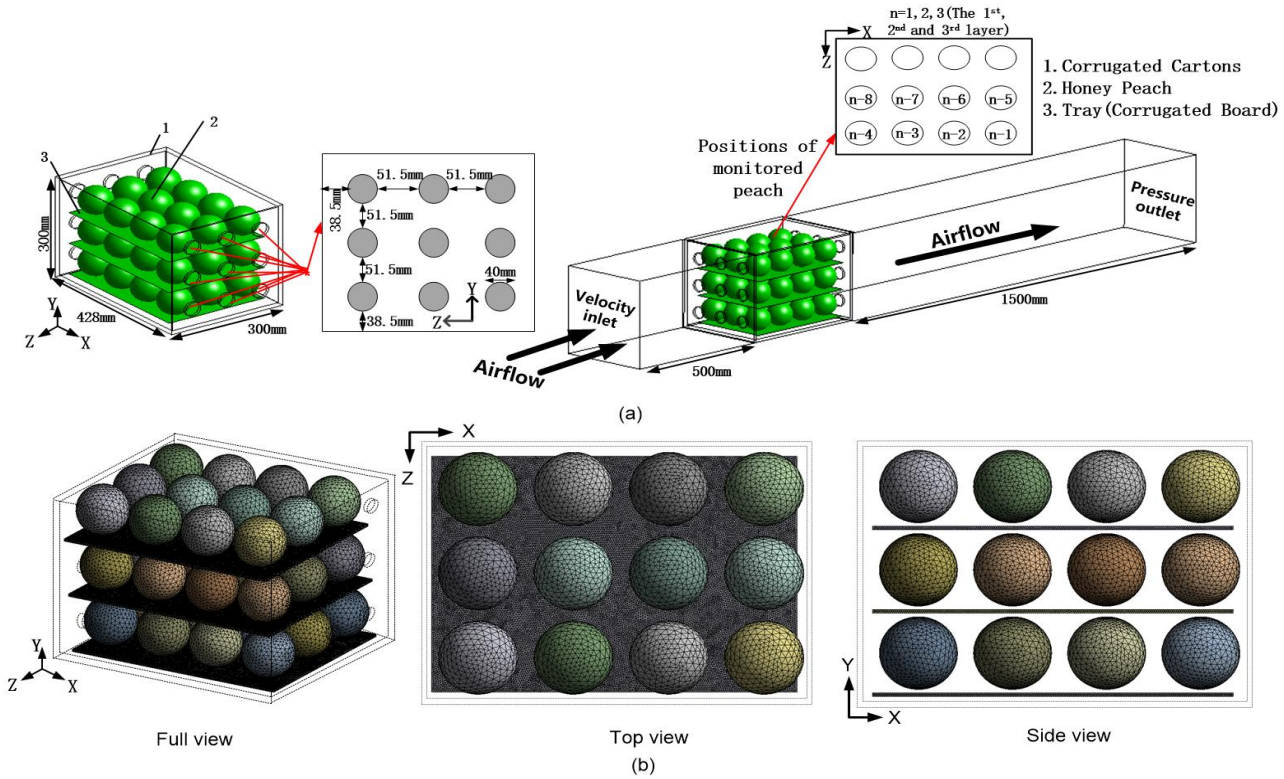

Fig. 1 - (a) Schematic diagram of precooling simulation: positions of monitored peaches inside an individual package *(from n-1 to n-8, where n=1,2,3)***, (b) computational grids of numerical model**

This model was divided into unstructured grids through Meshing software of ANSYS19.2. The number of grid cells after meshing in this model was about 6.93×10^6, with a space step of 1 mm. Through grid quality examination, the mesh skewness of this model was below 0.9, which presented a high and rational mesh quality of this model.

New modeling method of mathematical model

Assumptions in mathematical model: To simplify the mathematical model and facilitate the numerical calculation, necessary assumptions were made for the actual precooling process: The thermal-physical properties of peaches are constant, their heat conduction is isotropic, and their internal texture is uniform; Ignore the dissipating heat generated by the viscous dissipation; The precooling-air is regarded as an incompressible fluid with constant thermal properties; The precooling-air is considered to be a Newtonian fluid and a Boussinesq fluid.

Airflow and heat transfer model: For this study, we created a 3D model of peaches and air around it. The governing differential equations describing the fluid flow were solved with a general purpose fluid-flow solver (Fluent, ANSYS 19.2) in the 3D computational domain, which was divided into three parts: the air flow zone, the peach internal flow field and the coupling interfacial zone. The heat and momentum transfer in precooling process was performed with an unsteady state.

(1) The air flow zone

Mass conservation equation

$$\mathrm{div(U)}=0 \tag{1}$$

Momentum conservation equation:

$$\begin{aligned}
\rho_a\frac{\partial u}{\partial t}+\rho_a\mathrm{div(uU)}&=\mathrm{div}(\mu_a\mathrm{gradu})-\frac{\partial P_a}{\partial x}+S_u\\
\rho_a\frac{\partial v}{\partial t}+\rho_a\,\mathrm{div(vU)}&=\mathrm{div}(\mu_a\mathrm{gradv})-\frac{\partial P_a}{\partial y}+S_v\\
\rho_a\frac{\partial w}{\partial t}+\rho_a\mathrm{div(wU)}&=\mathrm{div}(\mu_a\mathrm{gradw})-\frac{\partial P_a}{\partial z}+S_w
\end{aligned} \tag{2}$$

Energy conservation equation:

$$\frac{\partial T_a}{\partial t}+\mathrm{div}(UT_a)=\mathrm{div}\left(\frac{\lambda_a}{\rho_a c_a}\mathrm{grad}T_a\right) \tag{3}$$

where: U is the velocity vector, u, v, w is the velocity component [m·s^{-1}] in the x, y, z direction, respectively. ρ_a and μ_a are the air density [kg·m^{-3}] and dynamic viscosity [Pa·s], respectively. c_a and λ_a are the air-specific heat capacity [J·kg^{-1}·K^{-1}] and thermal conductivity [W·m^{-1}·K^{-1}], respectively. P_a is water vapor pressure inside the carton [Pa], T_a is the air temperature [K], t is the precooling time for fruits [s]. S_u, S_v, S_w are generalized source terms in the x, y and z directions. Since air is an incompressible fluid, only the gravity effect of cold air is deemed to be $g=9.81$ [m·s^{-2}] in precooling, so $S_u=0$, $S_v=0$, $S_w=-\rho g$.

(2) Flow field internal to the peach

Heat sources internal to peaches (Q_{int}, [W·m^{-3}]) are mainly made up of respiration heat (Q_r, [W]) and transpiration heat (Q_t, [W]). Internal heat source is loaded into the heat conduction differential equation of the peach zone by an user-defined function (UDF) written in the C programming language.

$$\lambda_P\left(\frac{\partial^2 T_{P,t}}{\partial r^2}+\frac{2}{r}\frac{\partial T_{P,t}}{\partial r}+\frac{\cos\theta}{r^2\sin\theta}\cdot\frac{\partial T_{P,t}}{\partial\theta}+\frac{1}{r^2}\frac{\partial^2 T_{P,t}}{\partial\theta^2}\right)+Q_{int}=c_P\rho_P\frac{\partial T_{P,t}}{\partial t} \tag{4}$$

$$Q_{int}=\frac{Q_r-Q_t}{V_P} \tag{5}$$

where: $T_{p,t}$ is the peaches temperature at time t [K], c_P is peach-specific heat capacity [J·kg^{-1}·K^{-1}], λ_P and ρ_P are peach thermal conductivity [W·m^{-1}·K^{-1}] and density [kg·m^{-3}], respectively. V_P and A_p are the volume [m^3] and surface area of the peach [m^2].

Additionally, its heat of respiration and transpiration can be described as following formula (*Dehghannya et al., 2008*):

$$Q_r/V_P=\rho_P\times f_P \tag{6}$$

In this equation, f_p is the respiratory heat generation per unit mass of commodity [W·kg^{-1}], i.e., $f_P = (10.7/3600) \times m_1 \times [1.8(T_{P,t} - 273.15) + 32]^{m_2}$, where the respiration coefficients m_1 and m_2 are given in *Becker et al*. 2011 and successfully applied in many previous researches (*Delele et al. 2013a; Zhao et al. 2016*), i.e., 1.2996×10^{-5} and 3.6417 for peach.

$$Q_t/V_P = L_P m_P A_P/V_P = 3L_P m_P/r \quad (7)$$

Among them, $L_P = 9.1T_{P,t}^2 - 7512.9T_{P,t} + 3875100$, which presents evaporative latent heat [J·kg^{-1}], r is the vector radius of the peach (0.04 m).

When $P_p > P_a$ and $P_w > P_a$, $m_p = k_t(P_p - P_a)$, where k_t is the transpiration coefficient [kg·m^{-2}·s^{-1}·Pa^{-1}], and $P_p = VPL \cdot P_W$, $P_a = RH \cdot P_W$, $VPL = 0.99$ is the vapor pressure lowering effect of peaches (*Becker et al., 2011*) and $RH = 0.9$ is air relative humidity. P_P is the partial pressure of water vapor at the evaporating surface and P_W is the partial water vapor saturation pressure in air [Pa]:

$$P_W = \exp\left(23.4735 - \frac{3990.5}{T_a - 39.317}\right) \quad (8)$$

$$k_t = \frac{1}{1/k_a + 1/k_s} \quad (9)$$

where:

k_s and k_a are the skin mass-transfer coefficient and the air film mass-transfer coefficient, respectively, for peaches, k_s=14.2×10^{-9} [kg·m^{-2}·s^{-1}·Pa^{-1}] (*Becker et al., 2011*).

The value of k_t and k_a can be estimated by using the Sherwood- Reynolds-Schmidt correlations:

$$Sh = \frac{k_a \cdot 2r}{\delta M_{H_2O}} = 2.0 + 0.552Re^{0.53}Se^{0.33} \quad (10)$$

$$\delta = \frac{9.1 \times 10^{-9} \times T_a^{2.5}}{T_a + 245.18} \quad (11)$$

where:

δ is the diffusion coefficient of water vapor in air [m^2·s^{-1}].

Due to the low flow speed of the wet-cold air in the carton, $Re=0$ can be assumed (*Rennie et al., 2009*).

$$k_a = \frac{\delta M_{H_2O}}{R_{H_2O} T_a r} \quad (12)$$

For different precooling-air temperature, the values of δ, k_t and k_a were calculated by Eq. 9-12 and shown in Table 1.

$M_{H2O}=0.018$ is the molecular mass of water vapor [kg·mol^{-1}], $R_{H2O}=8.314$ is the water vapor constant [J·mol^{-1}·K^{-1}].

Table 1

Various parameters of different precooling-air temperature in simulation

Precooling-air temperature [°C]	Diffusion coefficient of water vapor	Air film mass transfer coefficient	Skin mass transfer coefficient
	δ ×10^{-5} [m^2·s^{-1}]	k_a ×10^{-9} [kg·m^{-2}·s^{-1}·Pa^{-1}]	k_t ×10^{-9} [kg·m^{-2}·s^{-1}·Pa^{-1}]
0	2.16490	4.28982	3.29454
2	2.19627	4.32035	3.31252
4	2.22784	4.35082	3.33040
6	2.25960	4.38123	3.34819
8	2.29155	4.41157	3.36588

(2) The coupling interfacial zone

According to the conservation of energy, the peach-air heat balance equation is obtained as (*Rennie et al., 2009*):

$$(\lambda_a \nabla T_a - \lambda_P \nabla T_{P,0}) n_{ap} = L_P (m_{con} - m_P) - \alpha_P (T_{P,0} - T_a) \quad (13)$$

where:

n_{ap} is an unit vector perpendicular to the peach-air interface,

α_P is the surface convective heat transfer coefficient of peach [W·m^{-2}·K^{-1}],

m_{con} is the condensation coefficient [kg·m^{-2}·s^{-1}].

Initial conditions and boundary conditions: The initial temperature of peach and the precooling-air temperature were set to 26 °C and 2 °C, respectively. The velocity-inlet boundary condition was used to define the airflow velocity at the inflow boundary (see Fig.1), and the airflow velocity was set to 2.5 m·s^{-1}. The pressure-outflow boundary condition was adopted at the outflow boundary. The surface of the peach, the inner and outer surfaces of the package, and the surface of trays were all taken as a no slip wall boundary.

Numerical simulation setting: Realizable k-ε turbulence model was used to simulate the whole precooling process. A pressure-based split solver was used, and the discrete format of momentum, energy, turbulent kinetic energy and diffusivity were set to second-order upwind scheme. We utilized semi-implicit method for pressure-linked equations (SIMPLE) to couple pressure to velocity, and used a transient simulation with a time step of 10 s and 20 iterations per time step.

The convergence criteria for continuity, momentum and turbulence were set to 10^{-4} and that for the energy equations was 10^{-6}. The thermal-physical parameters of each object in this model were shown in Table 2. The simulation was implemented in a 64-bit Windows10 computer with a 2.30 GHZ Inter®Core E5-2697 V4 CPU and 256GB RAM.

Table 2

Parameters of thermal-physical properties

Parameters	Density	Specific heat capacity	Thermal conductivity	Dynamic viscosity
	[kg·m^{-3}]	[J·kg^{-1}·K^{-1}]	[W·m^{-1}·K^{-1}]	[Pa·s]
Cooling air	1.293	1006	0.02343	1.73E-5
Honey Peach	691.95	3898.3	0.472	-
Corrugated Carton	220	1700	0.065	-
Tray (Corrugated Board)	260	1700	0.065	-

Parameters of precooling performance assessment

Cooling rate and SECT: The dimensionless temperature Y is used to analyse the cooling kinetics of the fruit. The formula for Y is expressed as (*Dincer, 1995):*

$$Y = \frac{T_{p,t} - T_a}{T_{P,0} - T_a} \quad (14)$$

where:

$T_{P,0}$ is the initial temperature of peaches (299.15 K).

The half (Y=1/2, HCT, min) cooling time is usually used to measure whether the fruit reaches the cooling average level.

The 7/8ths cooling time (Y=1/8, SECT, min) is used to measure whether the fruit is close to the commercial storage temperature.

The temperature of SECT is suitable for subsequent refrigerated transportation and storage. Therefore, the selection of SECT point is the most appropriate inflection point for refrigerated transfer.

Cooling uniformity: A variation curve of ΔY is a novel representation of cooling uniformity as a function with the dimensionless cooling time (Y_{avg}). Compared with temperature variability which has been reported as the relative standard deviation (*Defraeye et al., 2015*), the new heterogeneity index not only can observe the instantaneous uniformity (HI_t) at single time points, but also intuitively judge the overall heterogeneity index ($OHI=\Delta Y_{max}-\Delta Y_{min}$) by using a specific value.

A lower value of OHI represents a high level of temperature homogeneity, conversely, the worse precooling uniformity is (*Olatunji et al., 2017*):

$$Y_{avg,t} = \sum_{n=1}^{m} Y_{n,t} \Big/ m \tag{15}$$

$$\Delta Y_{n,t} = Y_{n,t} - Y_{avg,t} \tag{16}$$

$$HI_t = \Delta Y_{max-P,t} - \Delta Y_{min-N,t} \tag{17}$$

where:

$Y_{avg,t}$ is the average dimensionless temperature of all monitored fruits (n=24),

$\Delta Y_{max-P,t}$ and $\Delta\ Y_{min-N,t}$ are the maximum and minimum values of ΔY_n which reflects horticultural commodity higher or colder than the average temperature, thereby cooling slowly (hot spots) or faster (cold spots).

Moisture loss: Integrated evaluation of precooling efficiency is essential for optimizing cooling strategies of horticultural products and ensuring optimum fresh quality and safety. Thus, an influence of various precooling-air temperature on mass degradation should be taken into consideration.

$$-\frac{\partial M}{\partial t} = m_P \times A_P \tag{18}$$

Peaches mass loss (M, [mg]) mainly occurs by transportation driving force, which is estimated by Eq. 18 (*Hoang et al., 2003; Nalbandi et al., 2020*), among them, the rate of moisture loss m_p [kg·m^{-2}·s^{-1}] is calculated with Eq. 8-12.

Experimental verification

To determine the validity of this mathematical model, predicted (S_i) and measured (E_i) temperatures are compared based on the root-mean-square error ($RMSE$) and mean absolute percentage error ($MAPE$).

$$RMSE = \sqrt{\frac{1}{n}\sum_{i=1}^{n}(E_i - S_i)^2} \tag{19}$$

$$MAPE = \frac{1}{n}\sum_{i=1}^{n}\frac{|E_i - S_i|}{E_i} \times 100\% \tag{20}$$

Freshly Okubo peaches were harvested in July from Taigu of Shanxi Province (112º55′E, 37º43′N). Then peaches were immediately cooled in a self-made precooling device, where the precooling-air and relative humidity were set as 2℃ and 80-90%, respectively. At the same time, the air-inflow velocities were set to 0.7 and 2.7 m·s^{-1}, respectively.

The fruits' temperature was measured with a temperature digital recorder (SSN-13E, YOWEXA, Inc., Shenzhen, China). The accuracy of this sensor is ± 0.3℃. The fog making capacity of ultrasonic humidifier (HS-05-3, LUOSHE HUASHENG, Inc., Wuxi, China) is 0.3 KW.

RESULTS

Effect of air supply temperature on cooling rate

The effect of air supply temperature on cooling rate was examined by using the turbulence simulations for five different air supply temperatures: 0, 2, 4, 6 and 8℃. Fig. 2 compared the variation in the average temperature of peaches as a function of cooling time for different air supply temperatures.

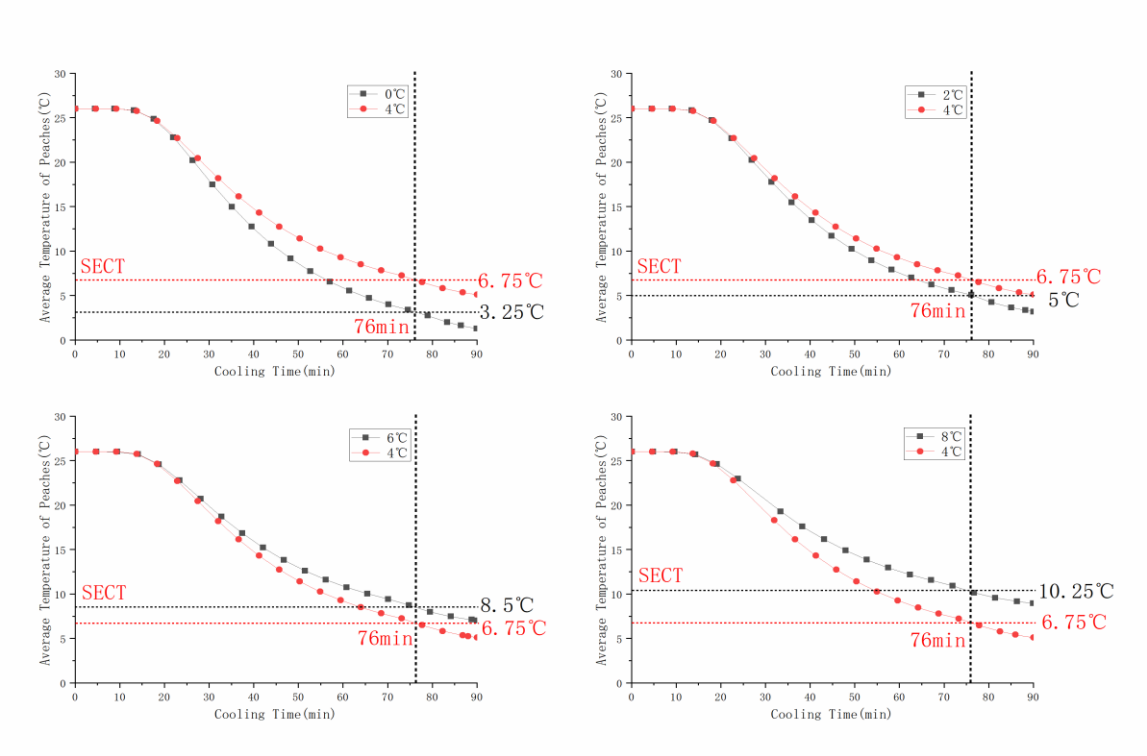

Fig. 2 - The average cooling temperature of peaches inside the container as a function of different air supply temperature: the monitoring position is the core temperature of peach

As it was clear in Fig. 2, its average temperature decreased gradually with the prolongation of cooling time. However, when air-inflow velocity was constant, the values of SECT did not increase as air supply temperature increased. For example, when air-inflow velocity was equal to 2.5 $m \cdot s^{-1}$, the SECT focused on ~76 mins. This meant that air supply temperature had no significant influence on the variations of SECT. This result was attributed to the fact that increasing the air supply temperature increased peaches transfer temperature in cold storage, and their transfer temperature was 3.25, 5, 6.75, 8.5 and 10.25°C, respectively, observed from Fig. 2. However, the substantial increase in air supply temperature made the precooling effect of fruit have certain limitations, especially for fruits (like peach) with high respiration intensity and perishability, which was mentioned in the following section. Therefore, we also needed to further study its corresponding variation trend of cooling time when the fruit was cooled from initial temperature (26°C) to fixed temperature on different precooling conditions. As could be seen from Fig. 3, the cooling time decreased with the decrease of air supply temperature, especially when its temperature was below 4°C, the variation range of cooling time was significantly reduced, as well as the same variation trend.

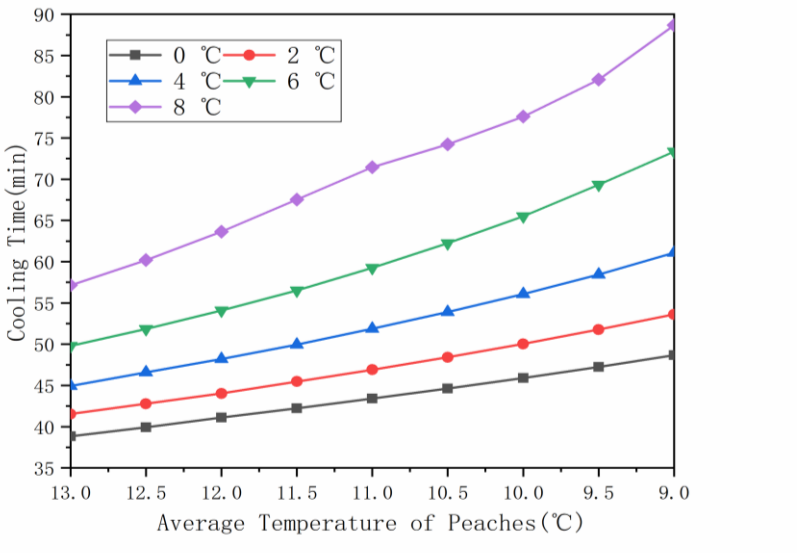

Fig. 3 - Relationship between air supply temperature and cooling time

In the actual precooling operation process, although too low air temperature shortened the cooling time, it was also easy to cause chilling injury to the fruit, thus affecting its sales quality. The specific magnitude of peaches chilling injury could be seen directly from Fig. 5, which showed the variation function curve of ΔY_{min} value and dimensionless temperature (Y_{avg}) at each precooling-air temperature.

According to Fig. 5, the maximum value of $|\Delta Y_{min}|$ at 8°C was 0.058, and the magnitude of its chilling injury effect was 30.12, 23.68, 17.14 and 9.38 % lower than other air supply temperatures (0-6°C). Based on this observation, blindly lowering the air supply temperature in precooling device gradually increased the chilling injury rate of peach. Therefore, it was recommended that the air supply temperature should not be lower than 2°C.

Effect of air supply temperature on cooling uniformity and quality loss

Observing Fig. 4, it was found that when air-inflow velocity was 2.5 $m \cdot s^{-1}$, the increase in air supply temperature gradually reduced the instantaneous temperature distribution gradient, namely, from 0.8 to 0.6℃. In addition, the curve variation trend of hot spot (ΔY_{max}) and cold point (ΔY_{min}) of the peach gradually developed as an "eye" shape (see Fig. 5), and its size also gradually decreased with the increase of air supply temperature, which was specifically reflected in the overall heterogeneous index value (OHI) of the peach inside the container, namely, 0.152, 0.137, 0.125, 0.117 and 0.106, respectively.

These analysis results fully demonstrated that its cooling uniformity was continuously improved with the increase of air supply temperature. Meanwhile, the overall heterogeneity index (OHI) of 8 °C is 30.26, 22.63, 15.20 and 9.40 % lower than other air supply temperatures (0-6 °C).

According to this result, air supply temperature of 4°C was a demarcation point that affected the uniformity of fruits. When air supply temperature was lower than 4°C, its size of "eye" increased significantly and asymmetrically. But when air supply temperature was increased to over 4°C, its variation range of "eye" was small and began to be distributed symmetrically.

This indicated that when air supply temperature exceeded 4°C, its temperature distribution began to be stable. Any further increase in air supply temperature did not improve the cooling uniformity obviously.

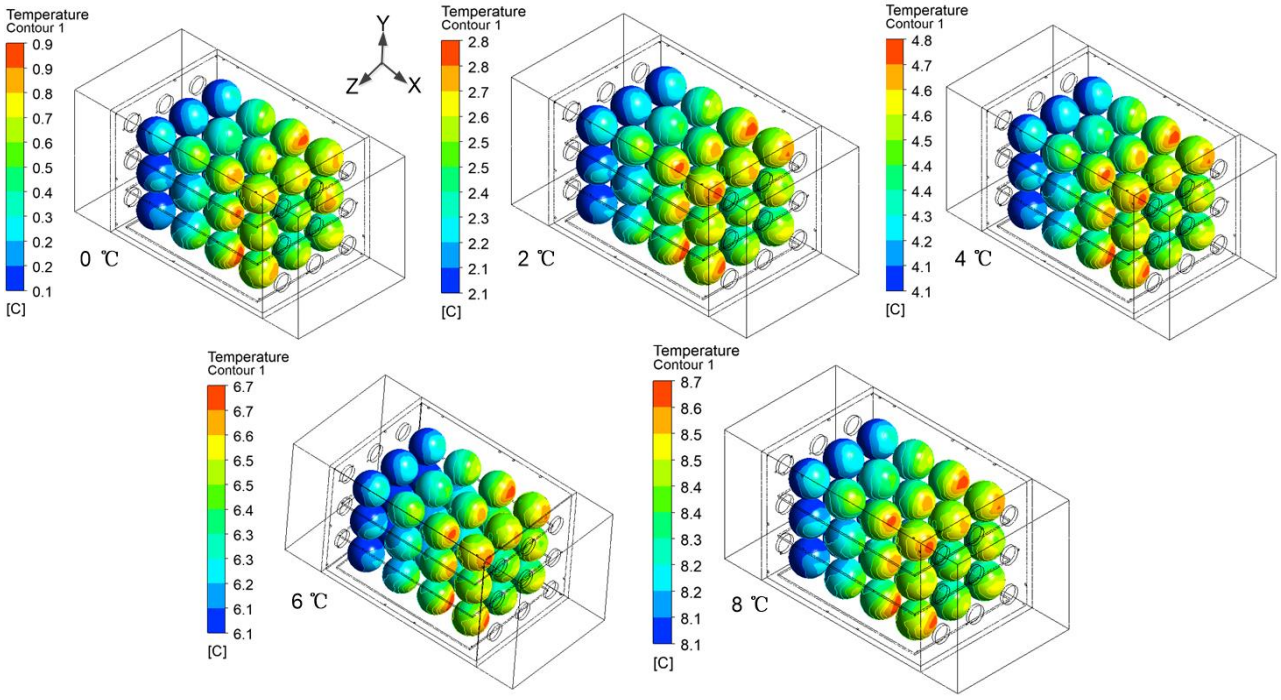

Fig. 4- Instantaneous static temperature (°C) contours of peaches inside an individual carton for different precooling-air temperatures at the simulation time of 90 min when air-inflow velocity is equal to 2.5 $m \cdot s^{-1}$

However, blind improvement of air supply temperature had a certain effect on the quality of peaches during precooling. This was because the increase of air supply temperature enhanced its respiration rate. For example, when the moment was at 90 mins, the instantaneous respiratory heat generated by peach per unit mass (f_p, calculated by Eq. 6) at 6-8°C is 0.041-0.053 $W \cdot kg^{-1}$, twice as much as that at 2-4 °C (0.022-0.027 $W \cdot kg^{-1}$) (see Fig. 6).

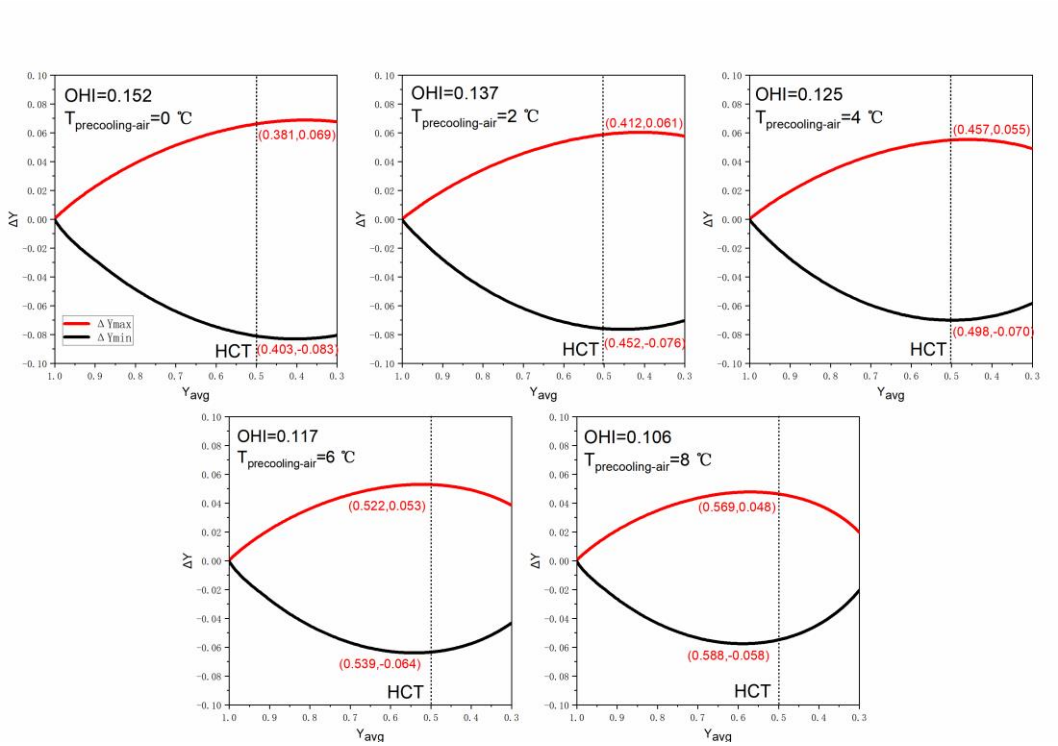

Fig. 5- Cooling heterogeneity curves of different precooling-air temperatures

Moreover, the continuous increase of respiration heat consumed fruit nutrients, accelerated its ripening speed and promoted the growth of microorganisms internal to the fruit, which was mentioned in previous study (*Dehghannya et al., 2012; Ngcobo et al., 2012*). These phenomena greatly improved peaches rotten rate, shortened their shelf life and commercial edible value. Meanwhile, the increase in respiration rate also increased their heat transfer resistance, forcing the cooling time to be prolonged continuously.

More importantly, the moisture loss at 2-4 °C was the lowest among that of all air supply temperatures (i.e., 73.85 and 76.61 mg), among them, the moisture loss at 6 °C was 39.74 and 34.71 % higher than that at 2 and 4°C. According to this result, the improvement of air supply temperature would reduce the taste and freshness of peaches. Thus, based on the comprehensive analysis of the above precooling performances, it was found that air supply temperature of 2-4 °C was the most appropriate range to maintain the quality of peaches during precooling.

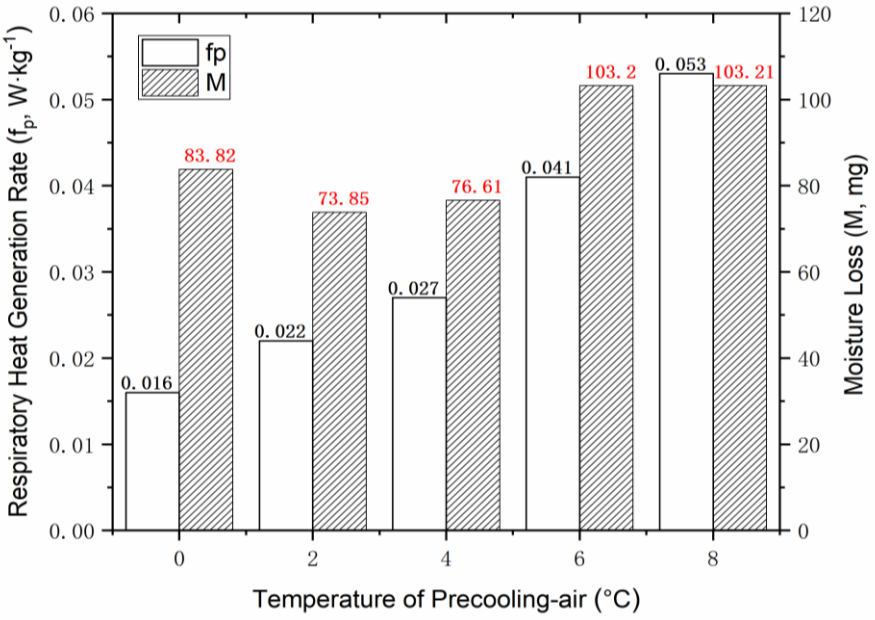

Fig. 6- Instantaneous respiratory heat generation rate (f_p) and cumulative moisture loss (M) at different precooling-air temperatures when peaches precooled for 90 mins

Validation of the established numerical model by experiment

The curve of experimental temperature and the simulated temperature were shown in Fig.7.

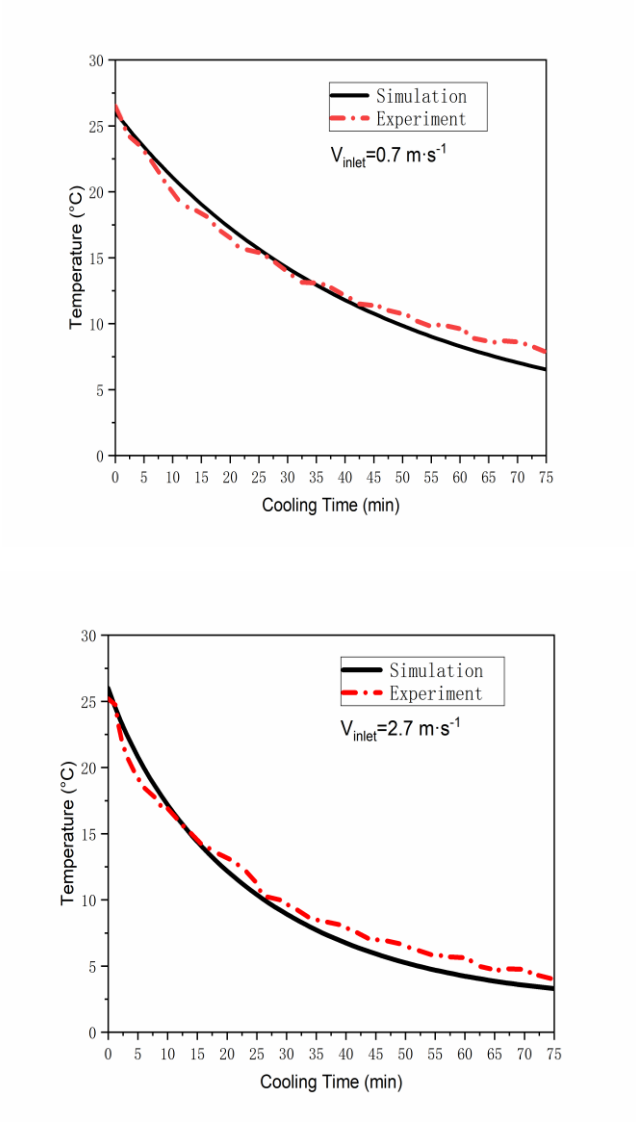

Fig. 7- Numerical simulation and experimental verification curve of peaches temperature with two air-inflow velocities: monitored position at peach 1-1

Overall, the simulated temperature was basically consistent with the measurement results. For the CFD model for 0.7 and 2.7 m·s^{-1}, their corresponding values of RMSE were 0.747 and 0.836 °C, respectively, as well as the MAPE values of 5.44 and 10.70%, respectively. The deviations could be considered satisfactory in view of the various parameters controlling the simulation and experiment. The results demonstrated that this new modeling method can predict the peaches convective heat transfer phenomenon accurately during the whole precooling process, thereby saving a lot of labour and material costs in the experiment.

CONCLUSIONS

In this study, the heat and mass transfer model of peaches forced air cooling (FAC) was established by CFD, and the heat source term was loaded into the Fluent model by UDF function. Then, the effect of various air supply temperatures on precooling performances was investigated and the following conclusions were obtained:

(1) The increase of air supply temperature had no remarkable effect on SECT when air-inflow velocity was constant, but significantly affected the cooling time when the air supply temperature exceeded 4 °C.

(2) In the actual precooling operation, too low air supply temperature resulted in higher chilling injury rate and poor cooling uniformity.

However, although the increase of air supply temperature could improve the cooling uniformity, it could also increase the respiration heat and moisture loss. Its respiration rate at 6-8 °C was about twice as high as that at 2-4 °C, and its corresponding moisture loss also increased by 34.71-39.74%. Thus, the air supply temperature in the range of 2-4℃ was proposed as optimum for quickly precooling peaches after harvest.

(3) This numerical model was highly consistent with the experiment (RMSE<1°C), so that this new modeling method with 3D simulator could be widely used for the simulation of precooling process of the peach, for which the cooling process inside the container was carried out in a turbulence airflow regime.

ACKNOWLEDGEMENTS

This work was funded by the National Key Research and Development Program of China (No. 2018YFD0700300).

REFERENCES

[1] Becker, B. R., Misra, A., Fricke, B. A., (2011), Bulk Refrigeration of Fruits and Vegetables Part I: Theoretical Considerations of Heat and Mass Transfer, *HVAC and R Research*, 2(2): 122-134.

[2] Berry, T. M., Defraeye, T., Nicolaï, B. M., Opara, U. L., (2016), Multi-parameter Analysis of Cooling Efficiency of Ventilated Fruit Cartons using CFD: Impact of Vent Hole Design and Internal Packaging, *Food and Bioprocess Technology*, 9(9): 1481-1493. https://doi.org/10.1007/s11947-016-1733-y

[3] Dincer, I., (1995), Air flow precooling of individual grapes, *Journal of Food Engineering*, 26(2): 243-249. https://doi.org/10.1016/0260-8774(94) 00049-F

[4] Dehghannya, J., Ngadi, M., Vigneault, C., (2008), Simultaneous Aerodynamic and Thermal Analysis during Cooling of Stacked Spheres inside Ventilated Packages, *Chemical Engineering Technology*, 31(11): 1651-1659.

[5] Dehghannya, J., Ngadi, M., Vigneault, C., (2012), Transport phenomena modelling during produce cooling for optimal package design: Thermal sensitivity analysis, *Biosystems Engineering*, 111(3): 315-324. https://doi.org/10.1016/j.biosystemseng.2012.01.001

[6] Delele, M. A., Ngcobo, M. E. K., Getahun, S. T., Chen, L., Mellmann, J., Opara, U.L., (2013a), Studying airflow and heat transfer characteristics of a horticultural produce packaging system using a 3-D CFD model. Part I: Model development and validation, *Postharvest Biology and Technology*, 86: 536-545. https://doi.org/10.1016/j.postharvbio.2013.08.014

[7] Delele, M. A., Ngcobo, M. E. K., Getahun, S. T., Chen, L., Mellmann, J., Opara, U.L., (2013b), Studying airflow and heat transfer characteristics of a horticultural produce packaging system using a 3-D CFD model. Part II: Effect of package design, *Postharvest Biology and Technology*, 86: 546-555. https://doi.org/10.1016/j.postharvbio.2013.08.015

[8] Defraeye, T., Cronjé, P., Berry, T., Opara, U.L., East, A., Hertog, M. & Nicolai, B., (2015), Towards integrated performance evaluation of future packaging for fresh produce in the cold chain, *Trends in Food Science & Technology*, 44(2): 201-225. https://doi.org/10.1016/j.tifs.2015.04. 008

[9] Ferrua, M.J., Singh, R.P., (2008a), Modeling the forced-air cooling process of fresh strawberry packages, Part II: Experimental validation of the flow model, *International Journal of Refrigeration*, 32(2): 349-358. https://doi.org/ 10.1016/j.ijrefrig.2008.04.009

[10] Ferrua, M.J., Singh, R.P., (2008b), Modeling the forced-air cooling process of fresh strawberry packages, Part III: Experimental validation of the energy model, *International Journal of Refrigeration,* 32(2): 359-368. https://doi.org/10.1016/j.ijrefrig.2008.04.011

[11] Hoang, M. L., Verboven, P., Baelmans, M., Nicolaï, B. M., (2003), A continuum model for airflow, heat and mass transfer in bulk of chicory roots, *Transaction of the ASAE*, 46(6): 1603-1611.

[12] Han, J.W., Qian, J.P., Zhao, C.J. & Fan, B.L., (2017), Mathematical modelling of cooling efficiency of ventilated packaging: Integral performance evaluation, *International Journal of Heat and Mass Transfer*, 111: 386-397. https://doi.org/10.1016/j.ijheatmasstransfer.2017.04.015

[13] Kummu, M., de Moel, H., Porkka, M., Siebert, S. & Ward, P.J., (2012), Lost food, wasted resources: Global food supply chain losses and their impacts on freshwater, cropland, and fertiliser use, *Science of the Total Environment*, 438: 477-489. https://doi.org/10.1016/j.scitotenv.2012.08. 092

[14] Norton, T., Sun, D. W., Grant, J., Fallon, R., Dodd, V., (2007), Applications of computational fluid dynamics (CFD) in the modelling and design of ventilation systems in the agricultural industry: A review, *Bioresource Technology*, 98(12): 2386-2414.

[15] Ngcobo, M.E.K., Delele, M.A., Opara, U.L., Zietsman, C.J. and Meyer, C.J., (2012), Resistance to airflow and cooling patterns through multi-scale packaging of table grapes, *International Journal of Refrigeration*, 35(2): 445-452. https://doi.org/10.1016/j.ijrefrig.2011.11.008

[16] Nalbandi, H., Seiiedlou, S., (2020), Sensitivity analysis of the precooling process of strawberry: Effect of package designing parameters and the moisture loss, *Food Science & Nutrition*, 8(5): 2458-2471. https://doi.org/10.1002/fsn3.1536

[17] Olatunji, J. R., Love, R. J., Shim, Y. M., Ferrua, M. J., East, A.R., (2017), Quantifying and visualising variation in batch operations: A new heterogeneity index, *Journal of Food Engineering*, 196: 81-93. https://doi.org/10.1016/j.jfoodeng. 2016.10.004

[18] Rennie, T.J., Tavoularis, S., (2009), Perforation-mediated modified atmosphere packaging: Part I. Development of a mathematical model, *Postharvest Biology and Technology*, 51(1) :1-9. https://doi.org/10.1016/j.postharvbio. 2008. 06. 007

[19] Wang, D., Lai, Y. H., Zhao, H.X., Jia, B.G. & Yang, X.Z, (2019), Numerical and Experimental Investigation on Forced-Air Cooling of Commercial Packaged Strawberries, *International Journal of Food Engineering*, 15(7). https://doi.org/10.1515/ijfe-2018-0384

[20] Zhao, C. J., Han, J. W., Yang, X. T., Qian, J. P., Fan, B. L., (2016), A review of computational fluid dynamics for forced-air cooling process, *Applied Energy*, 168: 314-331. https://doi.org/10.1016/j.apenergy.2016.01.101